

# Collective ratchet transport generated by particle crowding under asymmetric sawtooth-shaped static potential

Masayuki Hayakawa<sup>a,b</sup>, Yusuke Kishino<sup>b</sup>, and Masahiro Takinoue<sup>b,c</sup>

<sup>a</sup>RIKEN Center for Biosystems Dynamics Research, Kobe, Hyogo 650-0047, Japan; <sup>b</sup>Department of Computational Intelligence and Systems Science, Tokyo Institute of Technology, Yokohama, Kanagawa 226-8502, Japan; <sup>c</sup>Department of Computer Science, School of Computing, Tokyo Institute of Technology, Yokohama, Kanagawa 226-8502, Japan

## Supplementary Materials

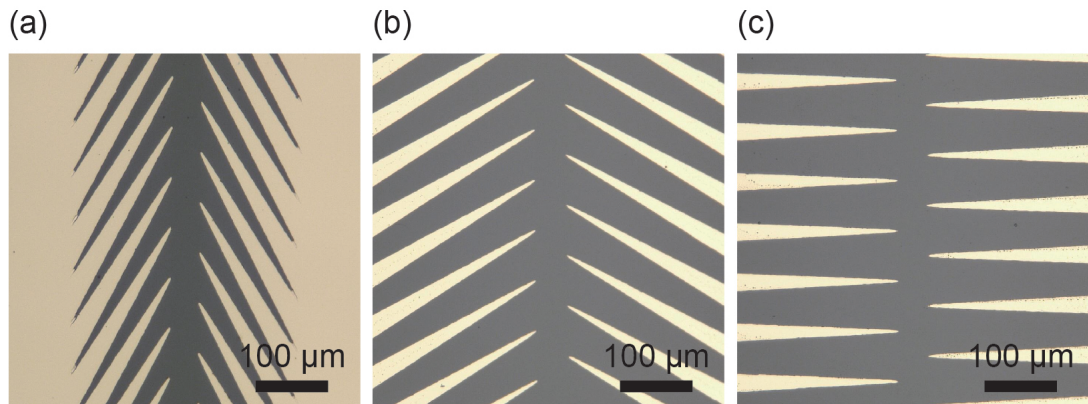


Figure S1: Sawtooth-shaped Au microelectrodes with various  $\theta$ . (a)  $\theta = 60^\circ$ , (b)  $\theta = 30^\circ$ , and (c)  $\theta = 0^\circ$ . At all conditions, the direct distance  $d$ , horizontal distance  $d_h$ , and vertical distance  $d_v$  between the tips of the sawtooth (defined in Fig. 1a) were  $53 \mu\text{m}$ ,  $40 \mu\text{m}$ , and  $70 \mu\text{m}$ , respectively.

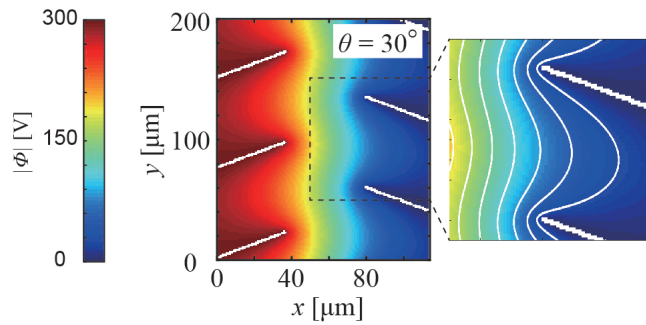


Figure S2: Calculated electric potential  $|\Phi|$  ( $\theta = 30^\circ$ ). The symmetricity along the  $y$ -axis is broken as in  $\theta = 60^\circ$  (Fig. 1b).

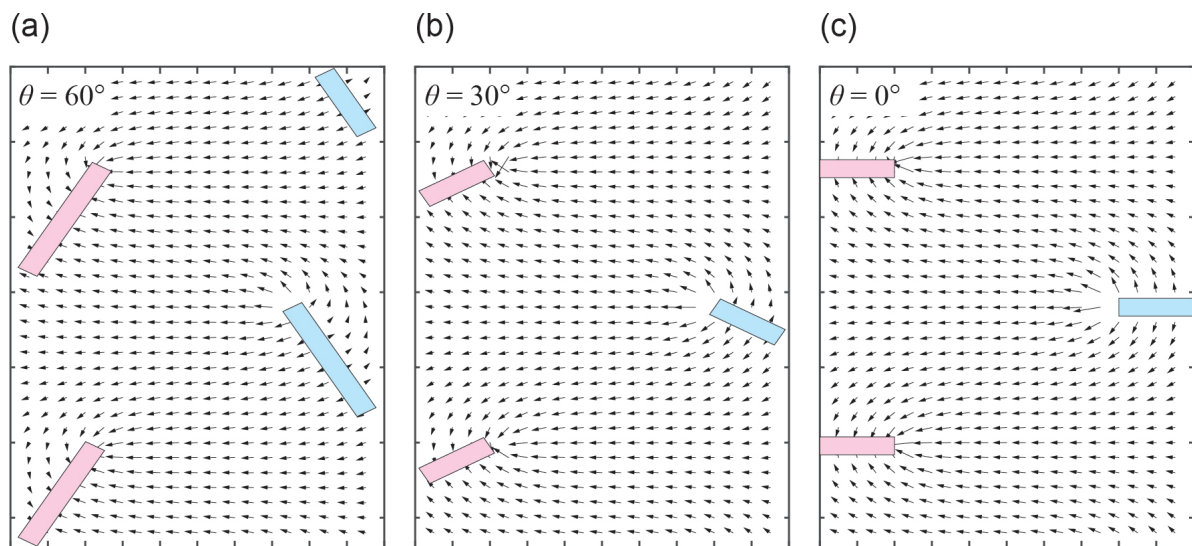


Figure S3: Calculated electric fields. Electric fields at (a)  $\theta = 60^\circ$ , (b)  $\theta = 30^\circ$ , and (c)  $\theta = 0^\circ$ . The red-colored sawtooth corresponds to the positive, whereas the blue-colored one is negative.

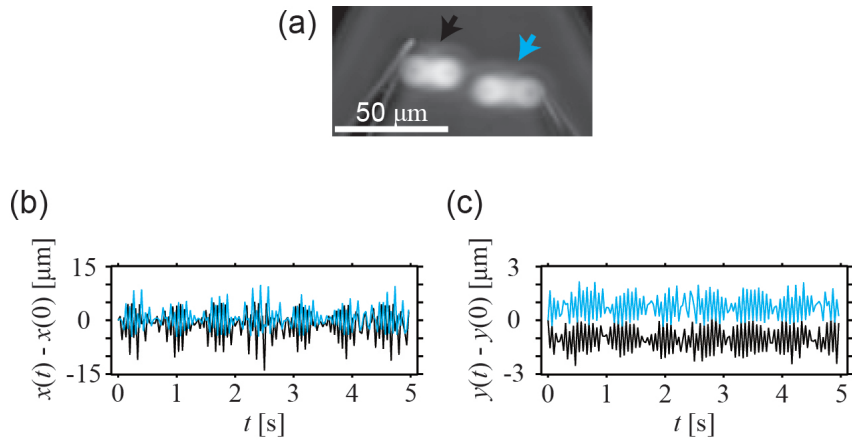


Figure S4: Motion of microparticles confined in between the tip of the sawtooth. (a) Maximum intensity projection image of the motions of two microparticles. The two microparticles collide with each other at the center of the electrode, eventually exhibiting back-and-forth motion. (b, c) Time variations of the  $x$  and  $y$ -coordinates of the two microparticles. As in the case of a single microparticle, both time variations oscillated. The color of each line corresponds to the color of the arrow in (a).

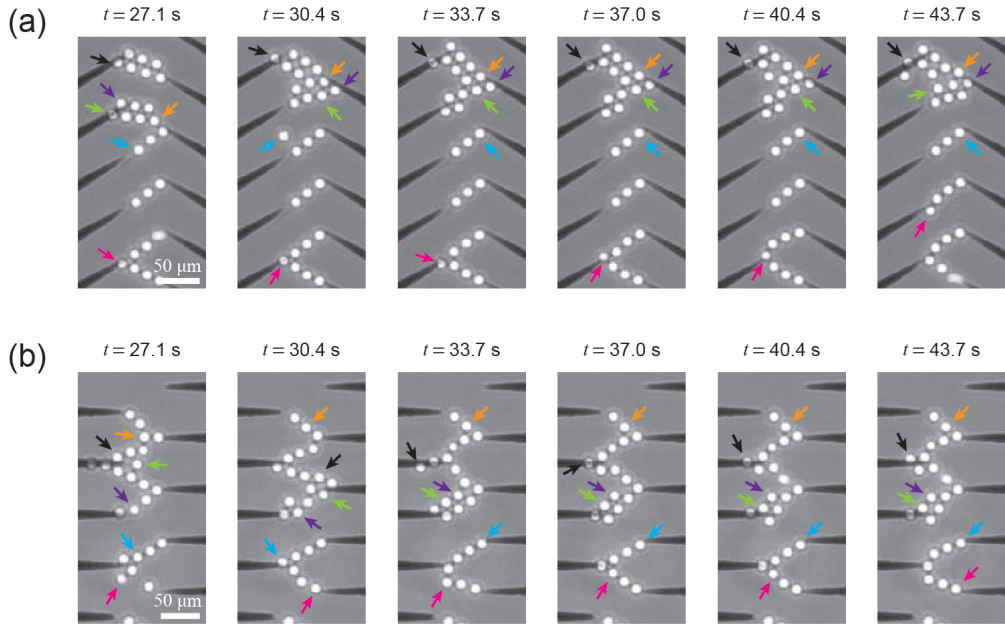


Figure S5: Motion of the crowded microparticles between the electrodes. (a) Collective transport of the microparticles between electrodes with  $\theta = 30^\circ$ . (b) Motion of the crowded microparticles between electrodes with  $\theta = 0^\circ$ . The arrow colors identify each microparticle.

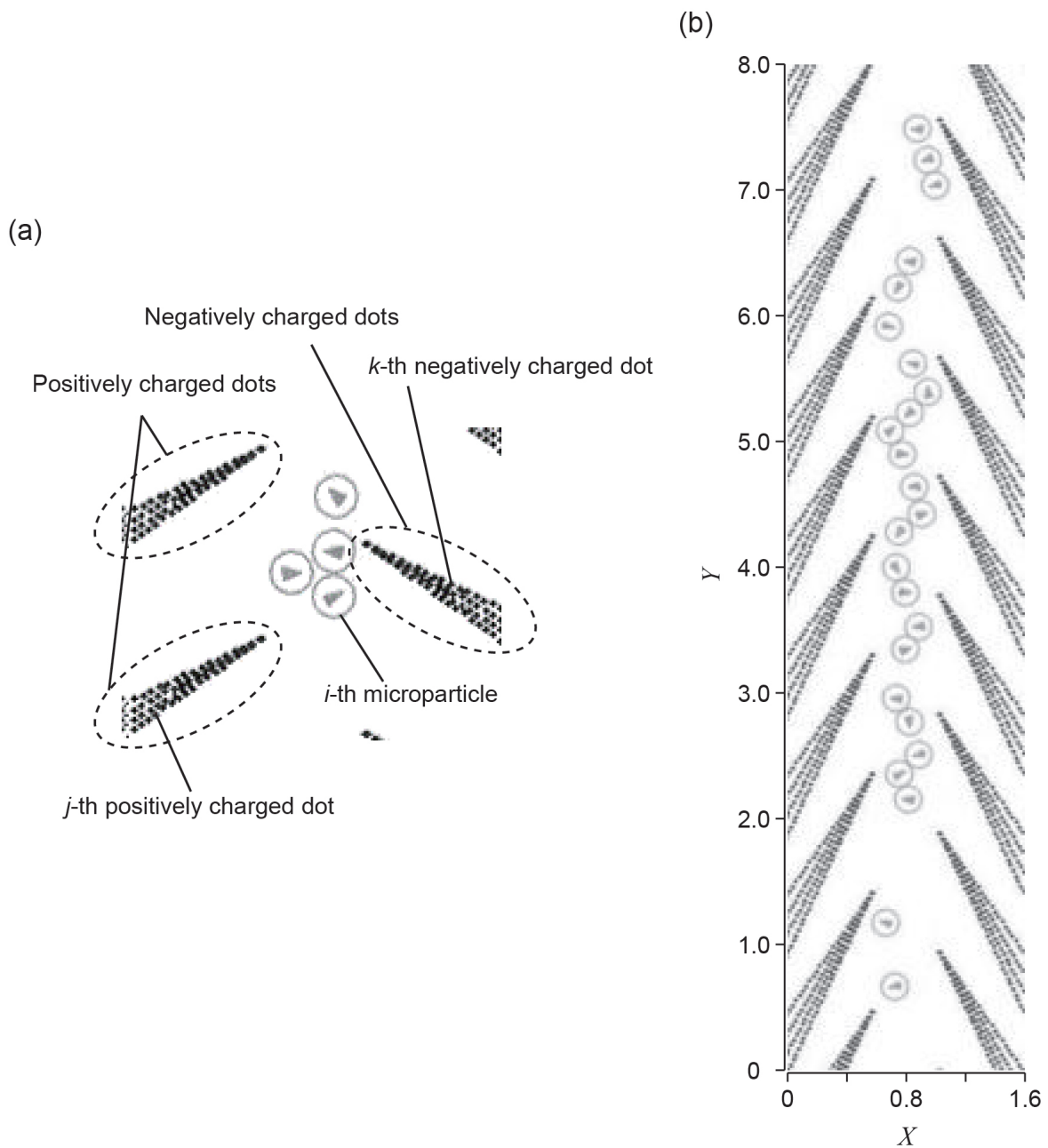


Figure S6: Picture of the microparticles and electrodes in the numerical simulation. (a) Arrowheads in the microparticles indicate the direction of motion. The electrode is represented by the patterned cluster of fixed dots with charge. (b) Original simulation window. The images in Figs. 3c and S7 were obtained by cropping the original simulation window.

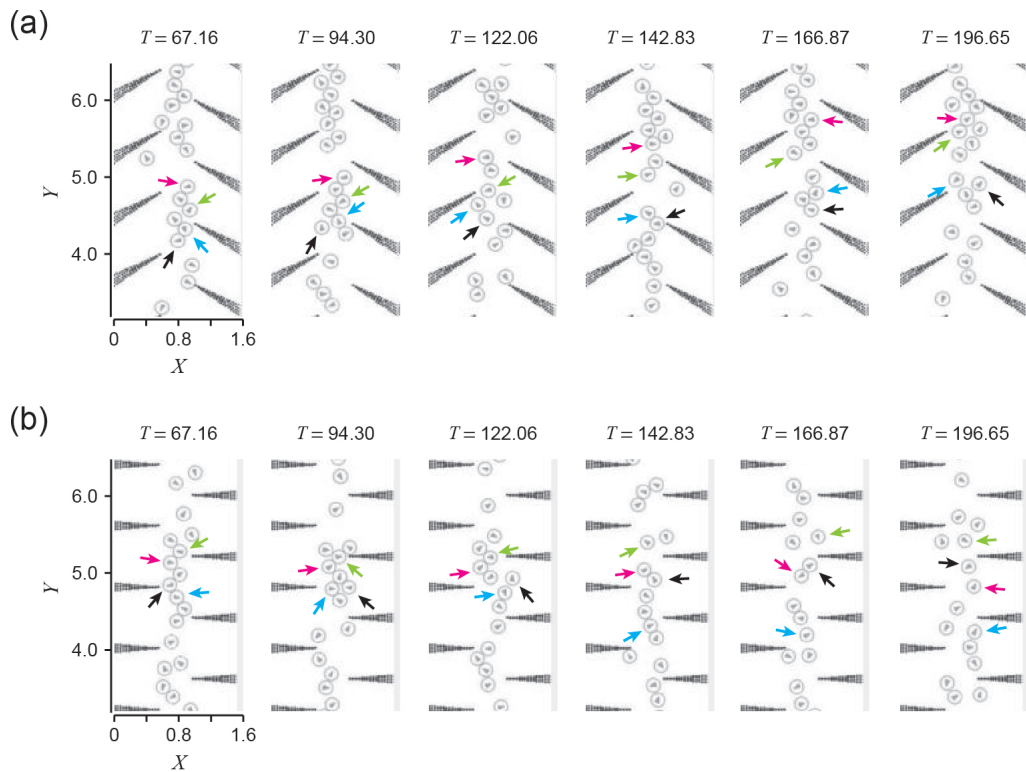


Figure S7: Numerical simulation of the microparticle motion. (a) Collective transport of the microparticles when  $\theta = 30^\circ$ . (b) Motion of the crowded microparticles when  $\theta = 0^\circ$ . The arrow colors identify each microparticle.

### Supplementary Note 1: Fabrication of the sawtooth-shaped Au electrode

A sawtooth-shaped Au electrode (Fig. 1a) was fabricated as follows. A glass slide (3.0 cm × 4.0 cm, Matsunami Glass, Japan) was initially baked at 150 °C for 15 min, and cleaned using a plasma cleaner (PIB-20, Vacuum Device, Japan). Further, using a spin coater (MS-A100, MIKASA, Japan), HMDS(1,1,1,3,3,3-Hexamethyldisilazane) (Wako Pure Chemical Industries, Japan) and S1818 photoresist (Dow Chemical, USA) were coated on the surface of the glass slide. The coated glass slide was then baked again at 115 °C for 1 min. The S1818 on the glass slide was exposed to UV light in a sawtooth pattern defined by a CAD file, using a direct laser exposure system ( $\mu$ PG101, Laser Pattern Generator, Heidelberg Instruments, Germany), and patterned S1818 was developed using an NMD developer (Tokyo-Ohka, Japan). Chromium and gold were deposited on the surface of the glass slide through vacuum vapor deposition (using VE-2012, Vacuum Device, Japan), after which the S1818 photoresist was removed by sonication in acetone (Wako Pure Chemical Industries, Japan). Finally, the ends of the sawtooth-shaped Au electrode were connected to ends of the wires using electroconductive glue (DOTITE D-723S, Fujikura Kasei, Japan).

## Supplementary Note 2: Calculation of the electric potential $|\Phi|$ and electric field $\mathbf{E}$

The electric potential  $|\Phi|$  and electric field  $\mathbf{E}$  attributed to the sawtooth-shaped electrode were obtained by solving a Laplace equation described below

$$\nabla^2(|\Phi|) = \frac{\partial^2|\Phi|}{\partial x^2} + \frac{\partial^2|\Phi|}{\partial y^2} = 0. \quad (1)$$

Here, the second order partial differentiations can be written as

$$\frac{\partial^2|\Phi|}{\partial x^2} = \frac{\frac{\partial}{\partial x}|\Phi(x + \Delta x, y)| - \frac{\partial}{\partial x}|\Phi(x, y)|}{\Delta x} = \frac{|\Phi(x + \Delta x, y)| - |\Phi(x - \Delta x, y)| - 2|\Phi(x, y)|}{\Delta^2 x}, \quad (2)$$

$$\frac{\partial^2|\Phi|}{\partial y^2} = \frac{\frac{\partial}{\partial y}|\Phi(x, y + \Delta y)| - \frac{\partial}{\partial y}|\Phi(x, y)|}{\Delta y} = \frac{|\Phi(x, y + \Delta y)| - |\Phi(x, y - \Delta y)| - 2|\Phi(x, y)|}{\Delta^2 y}. \quad (3)$$

Thus, the Laplace equation (eq.1) is represented as

$$|\Phi(x + \Delta x, y)| + |\Phi(x - \Delta x, y)| + |\Phi(x, y + \Delta y)| + |\Phi(x, y - \Delta y)| - \frac{1}{4}|\Phi(x, y)| = 0. \quad (4)$$

To solve eq.4 numerically, we replace  $x$  and  $y$  a lattice point  $i$  and  $j$ , then we obtain

$$|\Phi_{i,j}| = \frac{1}{4}(|\Phi_{i+1,j}| + |\Phi_{i-1,j}| + |\Phi_{i,j+1}| + |\Phi_{i,j-1}|). \quad (5)$$

We repeated to solve eq.5 until the solution converge. Initial condition was  $|\Phi| = 0$  (at the boundary and inside of the negative electrode) and  $|\Phi| = 300$  (at the boundary and inside of the positive electrode). And also, the electric field  $\mathbf{E}$  was calculated similarly using the obtained lattice of  $|\Phi|$ .

## Movie legends

- Movie S1: Back-and-forth motion of a single microparticle between a pair of sawtooth. Scale bar: 25  $\mu\text{m}$ .
- Movie S2: Stable alignment of three microparticles between a pair of sawtooth. Scale bar: 25  $\mu\text{m}$ .
- Movie S3: Collective ratchet transport observed in the experimental system ( $\theta = 60^\circ$ ). Image size: 174  $\mu\text{m} \times$  740  $\mu\text{m}$ .
- Movie S4: Collective ratchet transport observed in the experimental system ( $\theta = 30^\circ$ ). Image size: 174  $\mu\text{m} \times$  740  $\mu\text{m}$ .
- Movie S5: Motion of the microparticle crowding observed in the experimental system ( $\theta = 0^\circ$ ). Image size: 174  $\mu\text{m} \times$  740  $\mu\text{m}$ .
- Movie S6: Collective ratchet transport in the numerical simulation ( $\theta = 60^\circ$ ).
- Movie S7: Collective ratchet transport in the numerical simulation ( $\theta = 30^\circ$ ).
- Movie S8: Motion of the microparticle crowding in the numerical simulation ( $\theta = 0^\circ$ ).